Molecular Biology of the Cell
Vol. 18, 4979–4991, December 2007

The Golgin GCC88 Is Required for Efficient Retrograde Transport of Cargo from the Early Endosomes to the *Trans*-Golgi Network[D]

Zi Zhao Lieu,* Merran C. Derby,* Rohan D. Teasdale,† Charles Hart,* Priscilla Gunn,* and Paul A. Gleeson*

*The Department of Biochemistry and Molecular Biology and Bio21 Molecular Science and Biotechnology Institute, The University of Melbourne, Melbourne, Victoria 3010, Australia; and †Institute for Molecular Bioscience, The University of Queensland, Brisbane, Queensland 4072, Australia

Submitted June 29, 2007; Revised September 4, 2007; Accepted September 25, 2007
Monitoring Editor: Adam Linstedt

Retrograde transport pathways from early/recycling endosomes to the *trans*-Golgi network (TGN) are poorly defined. We have investigated the role of TGN golgins in retrograde trafficking. Of the four TGN golgins, p230/golgin-245, golgin-97, GCC185, and GCC88, we show that GCC88 defines a retrograde transport pathway from early endosomes to the TGN. Depletion of GCC88 in HeLa cells by interference RNA resulted in a block in plasma membrane–TGN recycling of two cargo proteins, TGN38 and a CD8 mannose-6-phosphate receptor cytoplasmic tail fusion protein. In GCC88-depleted cells, cargo recycling was blocked in the early endosome. Depletion of GCC88 dramatically altered the TGN localization of the t-SNARE syntaxin 6, a syntaxin required for endosome to TGN transport. Furthermore, the transport block in GCC88-depleted cells was rescued by syntaxin 6 overexpression. Internalized Shiga toxin was efficiently transported from endosomes to the Golgi of GCC88-depleted cells, indicating that Shiga toxin and TGN38 are internalized by distinct retrograde transport pathways. These findings have identified an essential role for GCC88 in the localization of TGN fusion machinery for transport from early endosomes to the TGN, and they have allowed the identification of a retrograde pathway which differentially selects TGN38 and mannose-6-phosphate receptor from Shiga toxin.

INTRODUCTION

Retrograde transport in the endocytic route to the *trans*-Golgi network (TGN) is important for the recycling of endogenous proteins such as mannose-6-phosphate receptor (M6PR), transmembrane peptidases such as furin, soluble *N*-ethylmaleimide-sensitive factor attachment protein receptors (SNAREs), TGN38/42, and the glucose transporter GLUT4 as well as the internalization of bacterial and plant toxins such as Shiga toxin and ricin (Ghosh *et al*., 1998, 2003; Lewis *et al*., 2000; Shewan *et al*., 2003; Sandvig and van Deurs, 2005; Bonifacino and Rojas, 2006). Several retrograde transport pathways from the endosomal compartments to the TGN have been identified (Sannerud *et al*., 2003; Bonifacino and Rojas, 2006). These include pathways from the late endosome to the TGN as well as from the early/recycling endosomes to the TGN. From biochemical and genetic analyses the machinery involved in the docking and fusion of transport intermediates with the TGN include tethering factors, small GTPases, and SNAREs (Sannerud *et al*., 2003; Bonifacino and Rojas, 2006); however, the identity of the components for each pathway remains poorly defined.

Several Golgi tethering molecules have been implicated in mammalian endosomal-to-TGN transport, including conserved oligomeric Golgi (Ungar *et al*., 2006), transport particle-II complex (Cai *et al*., 2005), and members of the golgin family (Tsukada *et al*., 1999; Lu *et al*., 2004; Yoshino *et al*., 2005). Our previous studies have focused on the role of a family of golgins specifically associated with TGN membranes in the regulation of membrane transport (Gleeson *et al*., 2004). There are four human TGN golgins, namely, p230/golgin-245, golgin-97, GCC185, and GCC88 (Kooy *et al*., 1992; Fritzler *et al*., 1995; Erlich *et al*., 1996; Gleeson *et al*., 1996; Griffith *et al*., 1997; Luke *et al*., 2003). These golgins are peripheral membrane proteins that have a TGN-targeting sequence located at the C terminus, called the GRIP domain (Barr, 1999; Kjer-Nielsen *et al*., 1999a; Munro and Nichols, 1999). Recruitment of p230/golgin-245 and golgin-97 to the TGN is mediated through an interaction with Arl1, a member of the ARF/Arl small G protein family (Gangi Setty *et al*., 2003; Jackson, 2003; Lu and Hong, 2003; Panic *et al*., 2003b). In contrast, the GRIP domains of GCC88 and GCC185, although dependent on G proteins for membrane binding, have different membrane binding properties from the GRIP domains of golgin-97 and p230/golgin-245 and they do not bind Arl1 in vivo (Derby *et al*., 2004), indicating different mechanisms of recruitment. Given that the four GRIP domain proteins form homodimers exclusively (Luke *et al*., 2005), each TGN golgin has the potential to function inde-

This article was published online ahead of print in *MBC in Press* (http://www.molbiolcell.org/cgi/doi/10.1091/mbc.E07–06–0622) on October 3, 2007.

[D] The online version of this article contains supplemental material at *MBC Online* (http://www.molbiolcell.org).

Address correspondence to: Paul A. Gleeson (pgleeson@unimelb.edu.au).

Abbreviations used: CI-M6PR, cation-independent mannose-6-phosphate receptor; Ecad, E-cadherin; M6PR, mannose-6-phosphate receptor; shRNA, short hairpin RNA; siRNA, small interfering RNA; STx-B, Shiga toxin B subunit; TGN, *trans*-Golgi network.

Supplemental Material can be found at:
http://www.molbiolcell.org/content/suppl/2007/10/19/E07-06-0622.DC1.html

pendently. Independent functions for each TGN golgin is supported by the observation that they are localized to distinct subdomains of the TGN (Luke *et al.*, 2003, 2005; Derby *et al.*, 2004; Lock *et al.*, 2005).

Recent studies have demonstrated a role for TGN golgins in both anterograde and retrograde membrane transport. The Arl1-dependent golgins, p230/golgin-245 and golgin-97, have been shown to be directly involved in anterograde transport from the TGN to the cell surface (Kakinuma *et al.*, 2004; Lock *et al.*, 2005). For example, E-cadherin is associated specifically with golgin-97 labeled tubules emerging from the TGN and depletion of golgin-97 blocks the exit of E-cadherin from the Golgi (Lock *et al.*, 2005). Several groups have reported that p230/golgin-245 and golgin-97 can also regulate membrane trafficking between the TGN and the endosomal system (Lu *et al.*, 2004; Yoshino *et al.*, 2005). The Arl 1-independent golgins GCC88 and GCC185 have received less attention than p230/golgin-245 and golgin-97, although evidence is emerging that these golgins also regulate trafficking. Recently, we showed that GCC185 is required both for the organization of the Golgi apparatus and for retrograde transport of Shiga toxin (Derby *et al.*, 2007). GCC185 depletion resulted in a block in Shiga toxin subunit B (STx-B) trafficking to the Golgi. In GCC185-depleted cells the internalized STx-B accumulated in Rab11-positive endosomes, indicating GCC185 was essential for transport between the recycling endosome and the TGN (Derby *et al.*, 2007). Interestingly, GCC185 did not seem to have an affect on TGN38 trafficking suggesting that Shiga toxin and TGN38 may use distinct retrograde transport pathways (Derby *et al.*, 2007). The question now arises whether different members of the TGN golgin family regulate separate retrograde transport pathways.

It is likely that GCC185 and GCC88 have distinct functions, because these two golgins are localized to distinct domains of the TGN (Derby *et al.*, 2004) and the expression of these full-length golgins perturbs the membranes of the TGN in a golgin-specific manner (Luke *et al.*, 2003; Derby *et al.*, 2004). In particular, by overexpressing these two golgins we noted that the recycling membrane protein TGN38 was associated with GCC88-labeled TGN membranes (Luke *et al.*, 2003) and excluded from GCC185-labeled membranes (Derby *et al.*, 2004). Given these earlier findings, we have now assessed the potential role of GCC88 in the retrograde transport of TGN38, Shiga toxin, and the mannose-6 phosphate receptor (M6PR). Using interference RNA, we show that depletion of GCC88 resulted in a block in retrograde transport of TGN38, and a fusion protein of M6PR, whereas transport of Shiga toxin to the TGN was unaffected. In GCC88-depleted cells, the cargo accumulated in the early endosomes. There are at least two SNARE complexes involved in retrograde transport from the early/recycling ensodomes to the TGN. Target membrane (t)-SNAREs, syntaxin 16, syntaxin 6, and Vti1a, which pair with the vesicle (v)-SNARE vesicle-associated membrane protein (VAMP)4 (or VAMP3) (Mallard *et al.*, 2002), and a syntaxin 5 complex with GS28 and Ykt6, which pairs with the v-SNARE GS15 (Xu *et al.*, 2002). Both complexes have been implicated in the retrograde transport of Shiga toxin (Mallard *et al.*, 2002; Tai *et al.*, 2004; Amessou *et al.*, 2007); however, the exact roles of these SNARE complexes in the individual pathways have yet to be established. Some of these syntaxins, particularly syntaxin 6 and syntaxin 5, are involved in more than one transport pathway (Wendler and Tooze, 2001; Tai *et al.*, 2004). Previously, we showed that the membrane structures resulting from the overexpression of full-length GCC88 included syntaxin 6 (Luke *et al.*, 2003), implying physical proximity between the two molecules. Here we have discovered that the depletion of GCC88 resulted in a perturbation of the intracellular distribution of syntaxin 6. The ability to rescue the trafficking defect of GCC88 depletion by overexpression of syntaxin 6 shows a direct link between the mislocalization of this t-SNARE and the block in retrograde transport. Our results suggest that GCC88 acts as an effector molecule to mediate the recruitment of SNARE molecules to the TGN.

MATERIALS AND METHODS

Plasmids, Antibodies, and Reagents

TGN38-cyan fluorescent protein (CFP) (Keller *et al.*, 2001) and E-cadherin-green fluorescent protein (Ecad-GFP) (Lock *et al.*, 2005) encode C-terminal fusion proteins with the fluorescent proteins. Untagged TGN38 was cloned into pIRES (Clontech, Mountain View, CA). GFP-Rab11 and GFP-Rab7(Q67L) are an N-terminal fusion with GFP, as described previously (Zhang *et al.*, 2004). Constructs encoding GFP-syntaxin 6 (Watson and Pessin, 2000) and GFP-full-length GCC88 (Luke *et al.*, 2003) have been described previously. The construct pCMU-CD8/cation-independent mannose-6-phosphate receptor (CI-MPR) encodes the extracellular and transmembrane domain of human CD8 α chain and the cytoplasmic domain of murine CI-MPR. Syntaxin 16 was polymerase chain reaction (PCR) amplified from HeLa cDNA and subcloned into pCherry-C1. Human autoantibodies to p230 (Kooy *et al.*, 1992) and early endosome associated protein 1 (EEA1) (Mu *et al.*, 1995) are as described previously. Monoclonal antibodies to GM130 and TGN38 were from BD Biosciences Transduction Laboratories (Lexington, KY). Monoclonal antibodies to human CD8α (clone PA-T8) were purchased from eBioscience (San Diego, CA). Monoclonal antibodies to syntaxin 6 were purchased from BD Biosciences (North Ryde, NSW, Australia). Mouse monoclonal anti α-tubulin was obtained from GE Healthcare (Rydalmere, NSW, Australia). Mouse monoclonal (2G11) antibodies to cation-independent mannose 6-phosphate receptor and rabbit polyclonal antibodies to VAMP3 and VAMP4 were purchased from Abcam (Cambridge, United Kingdom). Rabbit polyclonal antibodies to human GCC88 and GCC185 were described previously (Luke *et al.*, 2003). Rabbit polyclonal anti-human GMAP-210 has been described previously (Infante *et al.*, 1999), a gift from Michel Bornens (Curie Institute, Paris, France). Rabbit antibodies to Rab11 (Wilcke *et al.*, 2000) and Cys-3 conjugated STx-B (Mallard *et al.*, 1998) were gifts from Bruno Goud (Curie Institute). Rabbit polyclonal antibodies to syntaxin 16 (Mallard *et al.*, 2002) were generously supplied by Wangin Hong (IMCB, Singapore). HECD1, a mouse monoclonal antibody (from Dr. M. Takeichi, Kyoto University), was used to detect human E-cadherin. Secondary antibodies for immunofluorescence were sheep anti-rabbit immunoglobulin (Ig)-fluorescein isothiocyanate (FITC) and sheep anti-mouse Ig-FITC (Silenus Laboratories, Melbourne, Australia), whereas goat anti-rabbit IgG-Alexa Fluor 568, goat anti-rabbit IgG-Alexa Fluor 488, goat anti-mouse IgG-Alexa Fluor 647 nm and goat anti-human Alexa Fluor 594 nm were from Invitrogen (Carlsbad, CA). Horseradish peroxidase-conjugated sheep anti-rabbit Ig and anti-mouse Ig were from Dako North America (Carpinteria, CA).

Cell Culture and Transient Transfections

Cell lines were maintained as semiconfluent monolayer in DMEM supplemented with 10% (vol/vol) fetal calf serum (FCS), 2 mM L-glutamine, 100 U/μl penicillin, and 0.1% (wt/vol) streptomycin (C-DMEM) in a humidified 10% CO_2 atmosphere at 37°C. HeLa cells expressing a tetracycline-controlled transactivator (HeLa-tTa) (Gossen and Bujard, 1992) were maintained in 0.8 mg/ml Geneticin (G-418; Invitrogen). HeLa cells that stably express an inducible short hairpin RNA (shRNA) to GCC88 were grown in the abovementioned medium supplemented with 125 μg/ml zeomycin (Invitrogen). For transient transfections, HeLa cells were seeded as monolayers and transfected using FuGENE 6 (Roche Diagnostics, Basel, Switzerland) according to manufacturer's instructions. Transfections were carried out in C-DMEM at 37°C, 10% CO_2 for 24–96 h. Transient transfections with small interfering RNA (siRNA) were performed using Oligofectamine (Invitrogen), according to the manufacturer's instruction, for 72 h before analysis.

RNA Interference (RNAi)

The human golgin-97–specific siRNA duplex (Lu *et al.*, 2004), human GCC185-specific siRNA duplex (Reddy *et al.*, 2006), and siRNA duplex that targets both human and mouse p230/golgin-245 (Derby *et al.*, 2007) have been described previously. Human GCC88 was targeted with the specific siRNA (5′-GUCAGCAAUCUCAGGUAGA-3′) (Sigma Proligo, Lismore, Australia) and human syntaxin 6 with (5′-GUUGAAGCAAAUCCUAGAAdTdT-3′).

A short hairpin RNAi target to GCC88 was identified by the following criteria: potential target sequences were >75 nucleotides downstream of the start codon, target sequences did not contain a stretch of four or more A's or T's, and target sequences had a GC content close to 50%. The shRNA target

sequence to GCC88 used in this study is 5′-CTGCAGGCCATTCGAGATG-3′ (GCC88KD1). Oligonucleotides containing GCC88KD1 (Invitrogen) were designed for cloning according to manufacturer's instructions, with the exception that a nine-base pair hairpin loop sequence was used instead of the recommended four-base pairs loop sequence. Annealing of oligonucleotides was carried out by a stepwise temperature reduction and cloned into linearized pENTR/H1/TO vector (Invitrogen) according to the manufacturer's instructions to generate pENTR/H1/TO-shRNA$_{GCC88}$. A negative control shRNA with limited homology to any known sequence for human, mouse, and rat genome was obtained from Ambion (Applied Biosystems, Scoresby, Victoria, Australia).

Tetracycline-inducible HeLa Cells Expressing shRNA to GCC88

HeLa-tTa cells were passaged 24 h before transfection at a density of 2.5×10^5 cells per 75-cm^2 tissue culture flask. Monolayers were transfected with 5 μg of pENTR/H1/TO-shRNA$_{GCC88}$ by using FuGENE 6 according to manufacturer's instructions, and transfectants were selected in the presence of 125 μg/ml zeomycin for 10–14 d. Stable transfectants were cloned by limiting dilution and expression of shRNA induced by incubation with 10 ng/ml doxycycline (Sigma-Aldrich, Castle Hill, NSW, Australia), for 96 h. Depletion of GCC88 was analyzed by both indirect immunofluorescence and immunoblotting.

Indirect Immunofluorescence

Cells on coverslips were fixed with 4% paraformaldehyde for 15 min, followed by quenching in 50 mM NH_4Cl/phophate-buffered saline (PBS) for 10 min. Cells were permeabilized in either 0.1% Triton X-100/PBS or 0.1% saponin/PBS for 4 min and included in 5% FCS/PBS for 20 min to reduce nonspecific binding. Monolayers were incubated with primary and secondary conjugates described previously (Kjer-Nielsen *et al*., 1999b), and confocal microscopy was performed using a Leica TCS SP2 imaging system. For multicolor labeling, images were collected independently. For detection of cell surface E-cadherin (E-cad), cells were fixed and stained with anti-E-cad antibodies before permeabilization. Fluorescence intensity was analyzed using Leica confocal software (version beta 2000).

Internalization Assays

For TGN38 trafficking assays, stable HeLa A8 cells, or HeLa cells transfected with siRNA for 48 h, were transfected again with either TGN38-CFP or untagged TGN38 using FuGENE 6 (Roche Diagnostics, Indianapolis, IN) 24 h before the internalization assay. Cells were then incubated on ice for 10 min and washed twice with cold PBS. Mouse anti-rat TGN38, 1.25 μg/ml in serum-free media, was added, and the cells were incubated on ice for 30 min. Unbound antibodies were removed by washing and the internalization of antibody-bound TGN38 performed at 37°C for 30, 60 or 120 min, as described previously (Derby *et al*., 2007). Cells were fixed and permeabilized and the internalized TGN38–antibody complexes detected using Alexa Fluor 568-conjugated goat anti-mouse antibodies. The staining intensity of internalized TGN38 within the Golgi region was defined using the Golgi marker GMAP-210 and analyzed using Leica imaging software. Data were analyzed by an unpaired Student's *t*-test, two-tailed.

The Cy3-conjugated STx-B (Mallard *et al*., 1998) was bound on ice for 45 min, cells were washed, and then they were internalized continuously at 37°C for up to 2 h.

For CD8-M6PR internalization assays, HeLa A8 cells were incubated in C-DMEM containing 10 ng/ml doxycycline for 96 h to deplete GCC88 and transfected with pCMU-CD8-CI-M6PR by using FuGENE 6 (Roche Diagnostics) 24 h before the internalization assay. Monolyaers were incubated on ice for 10 min and washed with PBS. Monoclonal mouse anti-human CD8 antibodies (1.25 μg/ml in serum free media) were added on ice for 30 min. Unbound antibodies were removed and internalization of antibody-bound CD8-M6PR was carried out in serum-free medium for 60 min at 37°C. Monolayers were fixed in 4% paraformaldehyde and internalized CD8 molecules detected using Alexa Fluor 568-conjugated goat anti-mouse antibodies.

Immunoblotting

Cell extracts were dissolved in SDS reducing sample buffer, and samples were resolved on a 7.5% SDS-polyacrylamide gel electrophoresis (PAGE). Proteins were then transferred overnight onto an Immobilion-P transfer membrane (Millipore, NSW, Australia), and the membrane was dried at room temperature. The dried membrane was incubated with primary antibodies, diluted in PBS containing 1% (wt/vol) skim milk powder, for 1 h with rocking, followed by three 10-min washes in 0.05% Tween 20/PBS. Membranes were then incubated with peroxidase-conjugated anti-mouse or anti-rabbit immunoglobulin. Bound antibodies were detected by chemiluminescence (PerkinElmer Life and Analytical Sciences, Boston, MA), and images were captured and analyzed using the Gel Proanalyzer program (Media Cybernetics, Bethesda, MD).

RESULTS

Generation of Inducible Stable Cell Line Expressing shRNA to GCC88

Our previous studies demonstrated that the Arl1-independent TGN golgins GCC88 and GCC185 are recruited to distinct domains of the TGN (Derby *et al*., 2004). Given our recent findings that GCC185 is essential for retrograde transport of Shiga toxin (Derby *et al*., 2007), we investigated whether GCC88 is also involved in regulation of retrograde transport in this study. Two RNAi approaches were used to deplete intracellular GCC88 levels, namely, a vector-based shRNA system and siRNA. Initially, transient transfections of HeLa cells with pENTR/H1/TO-shRNA were used to identify an shRNA target sequence specific for GCC88. Once an RNAi target to GCC88 was identified, a stable HeLa cell clone (HeLa A8) expressing the tetracycline-inducible expression vector pENTR/H1/TO-shRNA was then generated. Cells were treated with doxycycline for 96 h to induce expression of the shRNA, and the subsequent depletion of GCC88 was analyzed by both indirect immunofluorescence and immunoblotting. Whereas GCC88 was readily detected by immunofluorescence in nontreated HeLa cells, very little GCC88 was detected in the HeLa A8 cell clone treated with either 10 or 100 ng/ml doxcyline for 96 h (Figure 1). Immunoblotting demonstrated that GCC88 protein was reduced in doxycycline-treated HeLa A8 cells by 90%, whereas the levels of other TGN golgins, namely, golgin-97 and GCC185, were unaffected (Figure 1B). HeLa A8 cells depleted of GCC88 remained viable for an extended period of >15 d.

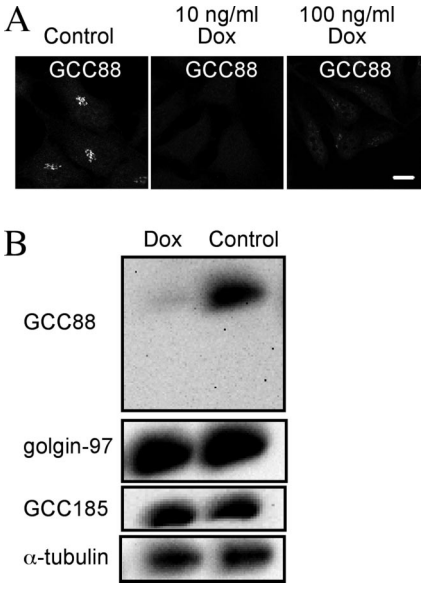

Figure 1. Depletion of endogenous GCC88 by an inducible shRNA. HeLa cells (clone A8) stably expressing a tetracycline^{on} inducible shRNA to GCC88 (tet^{R}GCC88KD A8) were either untreated (control) or treated with 10 or 100 ng/ml doxycycline (Dox) for 96 h, and monolayers were fixed with 4% paraformaldehyde. (A) Endogenous GCC88 was detected with rabbit anti-GCC88 antibodies followed by Alexa 488-conjugated anti-rabbit IgG. (B) HeLa A8 cells were incubated with 10 ng/ml doxycycline for 96 h, lysed in SDS-PAGE reducing buffer, and then extracts were subjected to SDS-PAGE on a 7.5% polyacrylamide gel. Proteins were transfer to a polyvinylidene difluoride membrane and probed with rabbit anti-GCC88 antibodies using a chemiluminescence detection system. The membrane were then stripped and reprobed with anti-α-tubulin, followed by anti-GCC185 and anti-golgin-97 antibodies. Bar, 10 μm.

The effect of GCC88-depletion on Golgi morphology was investigated using a number of Golgi markers. HeLa A8 cells were stained for endogenous GM130, a *cis*-Golgi marker, and p230/golgin-245 and γ-adaptin, TGN markers (Supplemental Figure S1). In both untreated and doxycycline-treated HeLa A8 cells, GM130, p230, and γ-adaptin retained a typical juxtanuclear Golgi staining pattern (Supplemental Figure S1), indicating that depletion of GCC88 did not disrupt Golgi structure.

Golgi Apparatus in GCC88-depleted Cells Is Functional

To determine whether the Golgi apparatus was functional in GCC88-depleted cells, anterograde transport of Ecad, a cargo protein localized to the plasma membrane was investigated. Untreated and doxycycline-treated A8 cells were transfected with Ecad-GFP, and, 24 h after the transfection, HeLa A8 cells were fixed and stained for endogenous GCC88. In both control and GCC88-depleted cells, Ecad-GFP showed plasma membrane, endosomal, and Golgi staining (Figure 2) reported previously (Lock *et al*., 2005; Lock and Stow, 2005). Cell surface Ecad was also readily detected by staining nonpermeabilized cells with anti-Ecad antibodies (Figure 2B); furthermore, the levels of surface Ecad seemed comparable between untreated and GCC88-depleted cells (ratio of cell surface-to-total fluorescence for control cells was 0.57 ± 0.15 and for GCC88-depleted cells was 0.63 ± 0.15). Similar results were obtained with a second membrane cargo molecule, namely, GFP-vesicular stomatitis virus G glycoprotein (data not shown). These data show that anterograde transport is functional in cells lacking GCC88 as cargo can be efficiently transported to the cell surface.

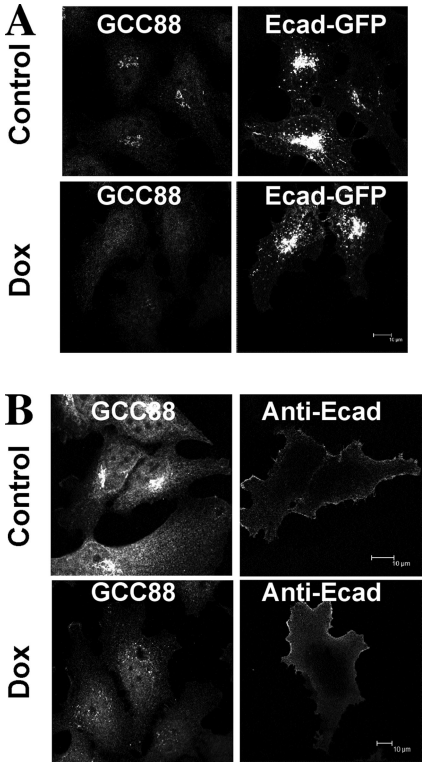

Figure 2. Anterograde transport of E-cadherin in GCC88-depleted cells is unaffected. HeLa A8 cells were either untreated (control) or incubated with 10 ng/ml Dox for 72 h and then transfected with Ecad-GFP for 24 h before staining. (A) Monolayers were fixed with 4% paraformaldehyde, permeabilized, and endogenous GCC88 was detected with rabbit anti-GCC88 antibodies followed by Alexa 568-conjugated anti-rabbit IgG and Ecad-GFP by GFP fluorescence. (B) Monolayers were fixed and stained with monoclonal anti-Ecad antibodies followed by Alexa 568-conjugated goat ant-mouse IgG. Fixed monolayers were then permeabilized and stained with rabbit anti-GCC88 antibodies followed by Alexa 647-conjugated goat anti-rabbit IgG. Bars, 10 μm.

TGN38 Recycling Is Blocked in GCC88-depleted Cells

We next examined whether retrograde transport was perturbed in cell lacking GCC88. Transport was initially investigated using two cargo molecules; TGN38, a membrane molecule that recycles continuously between TGN and the plasma membrane (Stanley and Howell, 1993; Ghosh *et al*., 1998), and STx-B, which is endocytosed and transported in a retrograde manner to the Golgi and then to the ER (Mallard *et al*., 1998).

Previously, we showed that endosome-to-TGN transport of STx-B requires the TGN golgin GCC185. To determine whether GCC88 also plays a role in the retrograde transport of this cargo, GCC88-depleted HeLa A8 cells were incubated with fluorescently tagged STx-B (Cy3-STx-B) for 45 min on ice, and then they were incubated at 37°C for up to 60 min. After the incubation, monolayers were washed, fixed, and stained for the Golgi marker GM130. In both untreated and doxycycline-treated HeLa A8 cells, STx-B was internalized into endosomal and Golgi structures by 20-min incubation at 37°C, and by 60 min it was found predominantly localized to Golgi apparatus (Figure 3). Therefore, depletion of GCC88 did not affect the retrograde transport of STx-B.

We next examined whether GCC88 may be required for endosome to TGN transport of TGN38. HeLa A8 cells were transfected with TGN38-CFP 24 h before an internalization assay. In noninduced cells, the TGN38–CFP fusion protein was detected predominantly within the Golgi region, and it was also detected at the plasma membrane and in punctate cytoplasmic structures, presumably endosomes (data not shown). In doxycycline-treated cells depleted of GCC88, TGN38-CFP had a similar intracellular distribution (data not shown). Although the steady-state distribution of TGN38 did not seem to be dramatically affected by GCC88 depletion, it is possible that GCC88 influences the rate of recycling of TGN38. To analyze the retrograde trafficking of TGN38 from the plasma membrane to the Golgi apparatus, anti-TGN38 antibodies were internalized at 37°C for up to 120 min, and the localization of the antibody–TGN38 complex was determined after fixation by staining with Alexa-conjugated anti-mouse IgG. As expected, the antibody–TGN38 complexes remained restricted to the cell surface at 4°C (Figure 4A, 0 min). In noninduced HeLa A8 cells, TGN38 was detected in an EEA1-positive compartment after 30 min at 37°C (Figure 4, A and B). Analysis of internalized TGN38 after either 30 or 60 min showed very little colocalization with GFP-Rab11 (Supplemental Figure S2), indicating that the transport pathway of TGN38 to the Golgi apparatus does not involve recycling endosomes. By 60 min, the majority of internalized TGN38 was detected in the Golgi of noninduced cells and by 120 min virtually all the antibody–TGN38 complexes were located in the Golgi region (Figure 4). In contrast, in GCC88-depleted cells the majority of internalized TGN38 was not transported to the Golgi over this period (Figure 5A). Rather, the internalized TGN38 remained in endosomal structures dispersed throughout the cytoplasm. Using GMAP-210 staining to mark the Golgi region, we quantified the immunofluorescence intensity of the internalized TGN38 that was located within the GMAP-

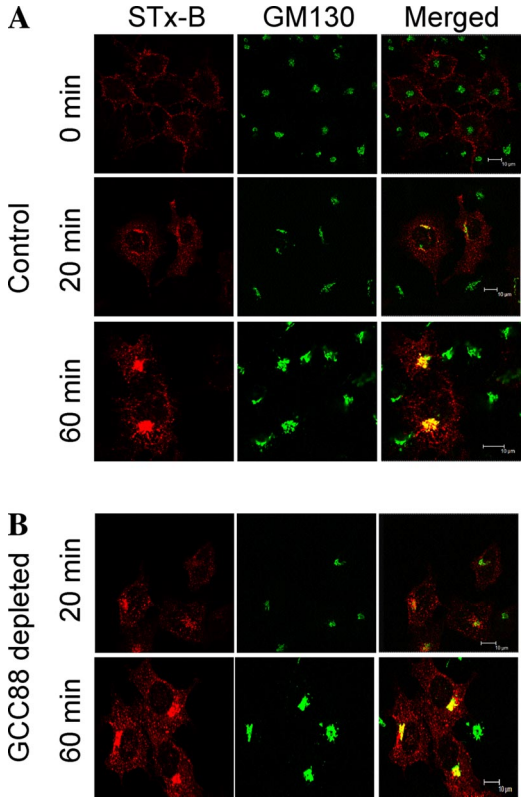

Figure 3. Shiga toxin is transported efficiently to the Golgi in GCC88-depleted cells. HeLa A8 cells were either untreated (control) (A) or incubated with 10 ng/ml doxycycline for 96 h (GCC88 depleted) (B). Monolayers were incubated with Cy3-conjugated STx-B for 45 min on ice, and then they were either fixed immediately (0 min) or incubated at 37°C for either 20 or 60 min, followed by fixation in 4% paraformaldehyde. Cells were stained with monoclonal antibodies to GM130 followed by Alexa-conjugated anti-mouse IgG. Bars, 10 μm.

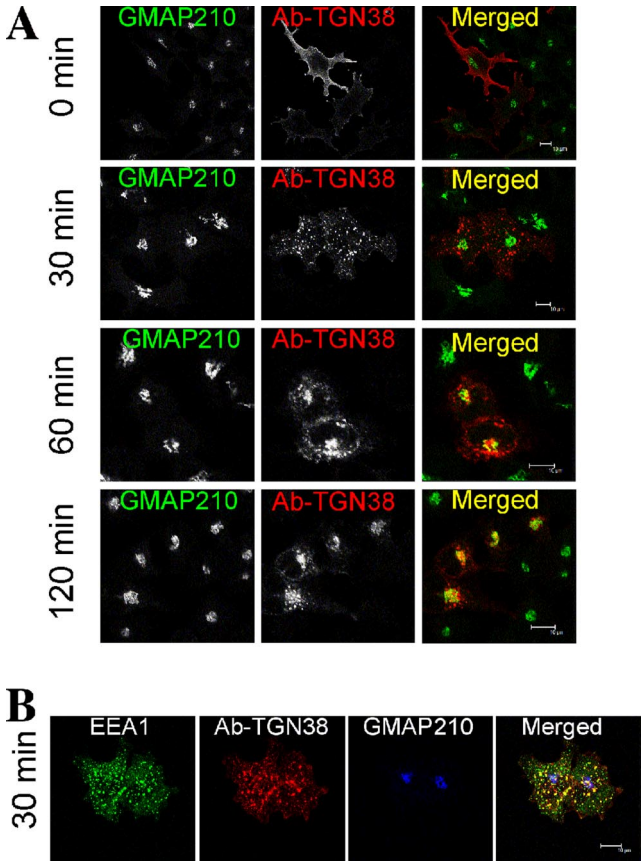

Figure 4. Retrograde transport of TGN38 in noninduced HeLa A8 cells. HeLa A8 cells were transfected with TGN38-CFP and 24 h later they were incubated with monoclonal mouse anti-TGN38 antibodies for 30 min on ice. After washing, cells were either fixed directly (0 min) or incubated at 37°C in serum-free media for the indicated time to internalize the antibody–TGN38 complex. (A) Monolayers were fixed in 4% paraformaldehyde, permeabilized, and stained with Alexa568-conjugated anti-mouse IgG for 60 min. Endogenous GMAP-210 was stained with rabbit anti-GMAP-210, followed by Alexa488-conjugated anti-rabbit IgG. (B) Monolayers were fixed and stained with anti-mouse IgG as in A and also stained with rabbit anti-GMAP-210, followed by Alexa647-conjugated anti-rabbit IgG and for EEA1 with human anti-EEA1 antibodies followed by FITC conjugated anti-human IgG. Bars, 10 μm.

210–stained Golgi region. After 60-min internalization GCC88-depleted cells had ~50% reduced level of TGN38 located in the Golgi region compared with untreated cells (Figure 5B) and after 120-min internalization a 35% lower level. By 4-h internalization (data not shown), the majority of surface TGN38 had recycled to the Golgi of GCC88-depleted cells, indicating that endosome–Golgi transport of this cargo did proceed but at a considerably slower rate than untreated HeLa cells. In contrast, a control shRNA had no affect on the kinetics of trafficking of surface TGN38 to the Golgi (data not shown).

To rule out the possibility of off-target affects by shRNA, doxycycline-treated HeLa A8 cells were transfected with a full-length GFP-tagged GCC88 construct (GFP-GCC88$_{FL}$) to determine whether overproduction of wild-type GCC88 would rescue the observed block in TGN recycling. In doxycycline-treated cells without exogenous GCC88, internalized TGN38–antibody complexes were found predominantly in endosomal structures after 120 min at 37°C, as expected. Analysis of the distribution of the TGN38–antibody complexes showed that in the majority of cells (23/25 cells) TGN38 was localized to endosomal structures and very little was detected in the perinuclear Golgi region (data not shown). However, in doxycycline-treated HeLa A8 cells expressing GFP-GCC88$_{FL}$, internalized TGN38 was predominantly Golgi-localized in all cells examined (>20 cells) after either 60 or 120 min at 37°C (Figure 5C), indicating that full-length exogenous GCC88 protein rescued the perturbation in TGN38 endosomal-to-Golgi trafficking.

To further rule out the possibility of off-target affects by shRNA, HeLa cells were also depleted of GCC88 by using an siRNA with a different target sequence to the shRNA. The majority (>90%) of GCC88 siRNA-transfected HeLa cells showed no or very weak staining for GCC88 (Figure 6A). siRNA depletion of GCC88 also resulted in a block in endosome to Golgi transport of TGN38 (Figure 6E). Consistent with the data from shRNA silencing, siRNA depletion of GCC88 resulted in the internalized TGN38–antibody complexes restricted to endosomal structures after a 120-min incubation at 37°C (Figure 6E). However, depletion of any of the other three TGN golgins, namely, p230/golgin-245, golgin-97, or GCC185 with siRNA had no affect on the retrograde transport of TGN38 to the Golgi (Figure 6, B–E). In each case, the siRNA was effective in depletion of the specific golgin (Figure 6, B–D), namely, for p230 siRNA ~85% of p230 siRNA-transfected HeLa cells showed minimal

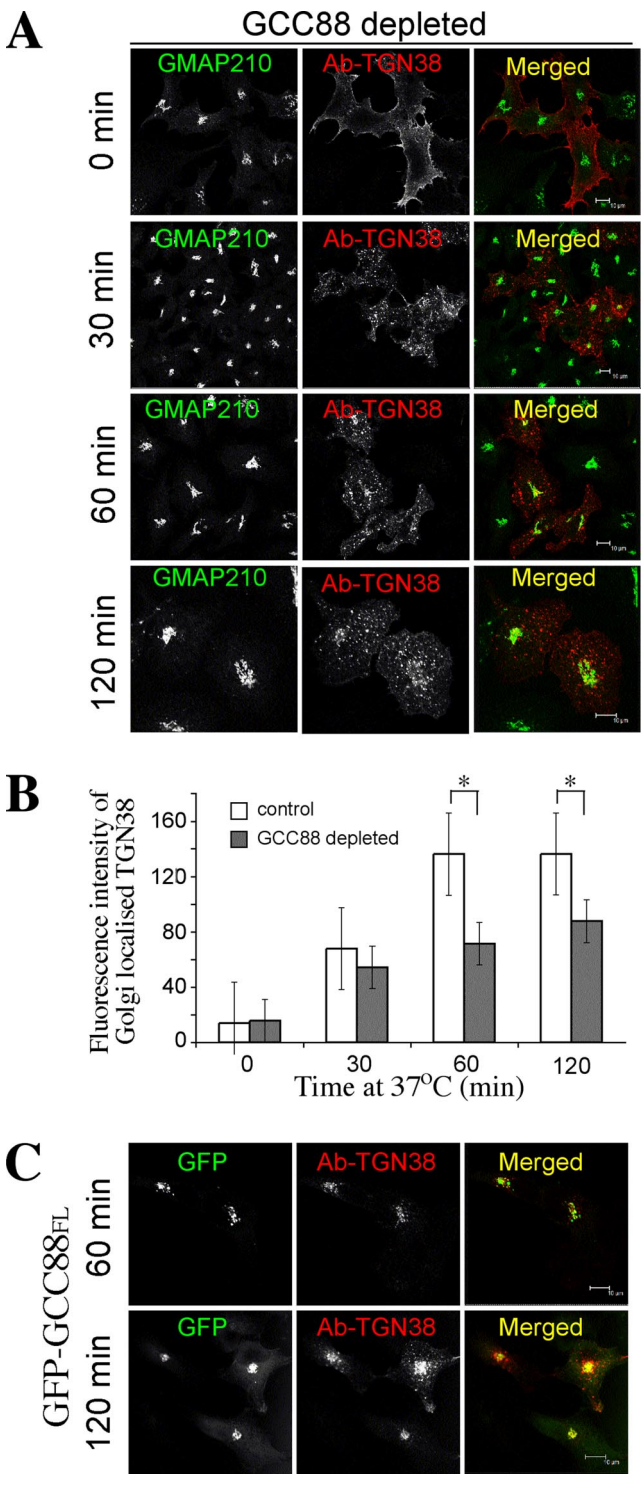

Figure 5. TGN38 trafficking is impaired in GCC88 depleted cells. (A) HeLa A8 cells were treated with 10 ng/ml doxycycline for 72 h, transfected with TGN38-CFP, and 24 h later they were incubated with anti-TGN38 antibodies at 0°C. After washing unbound antibodies, monolayers were either fixed directly (0 min) or incubated at 37°C for the indicated time to internalize the antibody–TGN38 complex, and then they were fixed in 4% paraformaldehyde and permeabilized. Cells were stained with Alexa568-conjugated anti-mouse IgG. Endogenous GMAP-210 was stained with rabbit anti-GMAP-210, followed by Alexa488-conjugated anti-rabbit IgG. (B) GCC88-depleted cells were stained as described above, and TGN38 staining intensity within the Golgi region was determined using GMAP-210 staining to mark the Golgi location. Fluorescence intensity was quantified using Leica imaging software (n = 25 for each time point). Results are means and error bars represent standard deviation. *P < 0.001. (C) HeLa A8 cells were incubated with 10 ng/ml doxycycline for 96 h, and then they were transfected with TGN38 together with GFP-GCC88$_{FL}$ 24 h before an internalization assay. Monolayers were incubated with monoclonal anti-TGN38 antibodies for 30 min on ice, washed in PBS, and then incubated at 37°C in serum-free media for either 60 or 120 min, as indicated. Monolayers were fixed in 4% paraformaldehyde, permeabilized, and stained with Alexa568-conjugated anti-mouse IgG. GFP-GCC88$_{FL}$ was detected by GFP fluorescence. Bars, 10 μm.

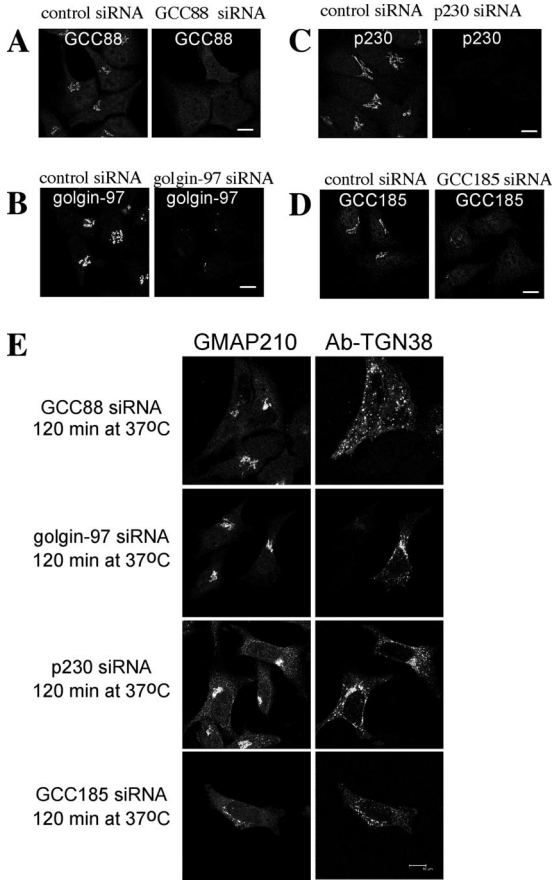

Figure 6. TGN38 trafficking in inhibited by silencing GCC88 but not the other TGN golgins. HeLa cells were transfected with GCC88 siRNA (A), golgin-97 siRNA (B), p230 siRNA (C), and GCC185 siRNA (D) for 72 h, fixed in 4% paraformaldehyde, and stained with rabbit anti-GCC88 antibodies, monoclonal mouse anti-golgin-97 antibodies, human anti-p230 antibodies, and rabbit anti-GCC185 antibodies, respectively, followed by Alexa568-conjugated IgG. (E) HeLa cells transfected with siRNA as described above for 48 h and then transfected a second time with TGN38-CFP for a further 24 h. Monolayers were then incubated with monoclonal mouse anti-TGN38 antibodies on ice for 30 min, washed with PBS, and incubated in serum-free media at 37°C for 120 min. Monolayers were fixed in 4% paraformaldehyde, permeabilized, and stained with Alexa568-conjugated anti-mouse IgG. Endogenous GMAP-210 was stained with rabbit anti-GMAP-210, followed by Alexa488-conjugated anti-rabbit IgG. Bars, 10 μm.

staining for p230; for golgin-97 siRNA ~70% of golgin-97 siRNA-transfected HeLa cells showed minimal staining for golgin-97; and for GCC185 siRNA ~85% of GCC185 siRNA-

transfected HeLa cells showed minimal staining for GCC185. In each case, internalized TGN38–antibody complexes were trafficked efficiently to the Golgi apparatus, as indicated by the use of the Golgi marker GMAP-210 (Figure 6E). Whereas depletion of golgin-97 and p230 does not significantly perturb the Golgi structure, GCC185 depletion results in Golgi fragmentation (Figure 6E), as reported previously (Derby *et al*., 2007). Nonetheless, the TGN38–antibody complexes were efficiently trafficked to the GMAP-210–positive structures in GCC185-depleted cells (Figure 6E). Quantitative analysis of p230, golgin-97 and GCC185 siRNA transfections showed that internalized TGN38–antibody complexes were localized to Golgi structures in >75% of transfected cells. Together, these data clearly exclude off-target affects of the GCC88 RNAi and they strongly suggest that the inhibition of TGN38 trafficking in GCC88-depleted cells is specific for this particular TGN golgin.

TGN38 Is Blocked in an EEA1-positive Compartment

Internalization of TGN38 in GCC88-depleted cells was further investigated to determine the site of the cargo block. In doxycycline-treated HeLa A8 cells, the internalized TGN38–antibody complexes showed extensive colocalization with endogenous EEA1, even after 120 min at 37°C (Figure 7A). Fluorescence intensity profiling further demonstrates the degree of overlap, where in the majority of cases peaks of fluorescence containing the TGN38–antibody complex show coincidence with EEA1 (Figure 7B). In contrast, internalized TGN38 showed minimum colocalization with GFP-Rab7 (late endosomes) or GFP-Rab11 (recycling endosomes) (Figure 7C). These data indicate that GCC88 is required for the retrograde transport of TGN38 from the early endosome to the TGN.

GCC88 Is Required for Plasma Membrane Recycling Mannose-6-Phosphate Receptor Fusion Protein

To determine whether a deficiency of GCC88 affected retrograde transport of other membrane cargo molecules, we analyzed the trafficking of the CI-M6PR. First, we assessed the steady-state distribution of the endogenous CI-M6PR in HeLa A8 cells. In noninduced A8 cells, the majority of the CI-M6PR was localized predominantly to a perinuclear location, and it showed significant colocalization with GCC88 (Figure 8), consistent with the localization of this receptor in the TGN (Ghosh *et al*., 2003). However, in GCC88-depleted cells, CI-M6PR was distributed in cytoplasmic structures. These CI-M6PR cytoplasmic structures showed extensive colocalization with EEA1, but not with Rab7(Q57L) or Rab11 (Supplemental Figure S3). We quantified the fluorescence intensity of CI-M6PR found located within the Golgi region by using GMAP-210 staining to mark the location of the Golgi apparatus. Analysis of the fluorescence intensity revealed that there was >50% reduction of CI-M6PR in the Golgi region of GCC88-depleted cells compared with untreated cells (Figure 8B). These data indicate that the trafficking of endogenous CI-M6PR is perturbed in the absence of GCC88 and accumulates predominantly in early endosomes.

Next, we followed the trafficking of CI-M6PR. Here, we have used a CD8-M6PR chimera, because this chimera can be tagged at the plasma membrane by staining against CD8 and the trafficking of the internalized CD8-M6PR chimera–antibody complex then assessed. Previous studies have demonstrated that a similar CD8-M6PR chimera was transported to the TGN via the early endosomes (Seaman, 2004). HeLa A8 cells were transfected with CD8-M6PR for 24 h before an internalization assay. To analyze the trafficking of

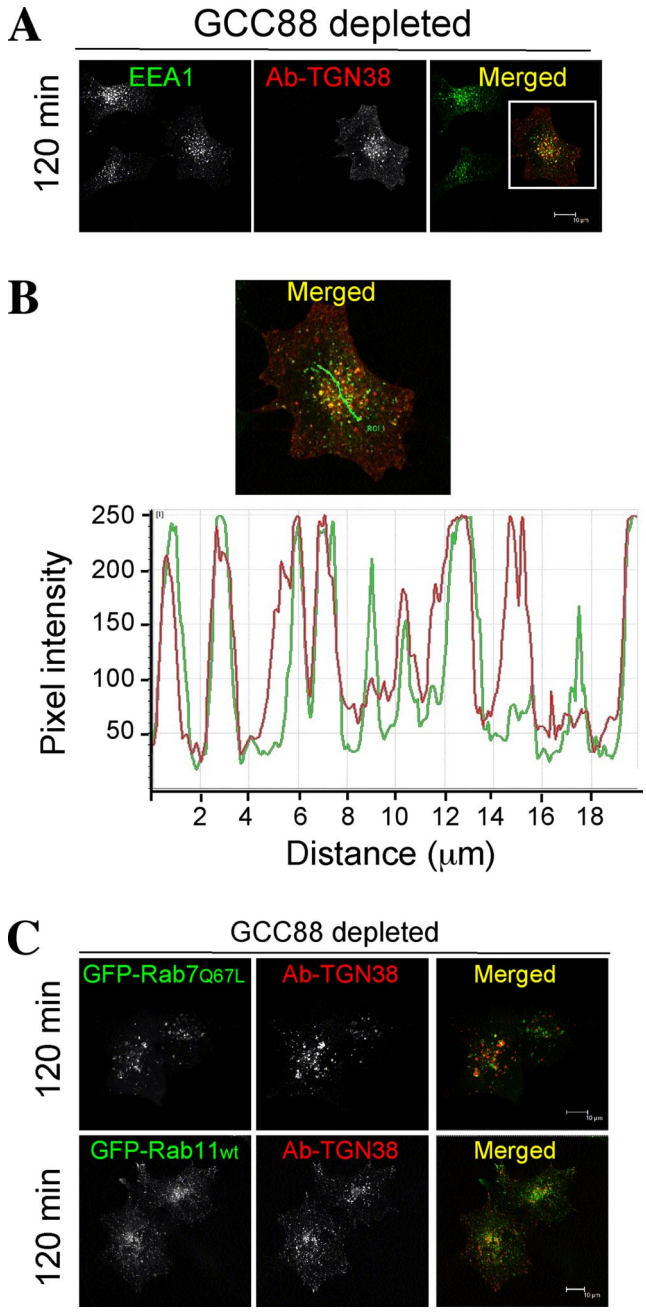

Figure 7. Internalized TGN38 accumulates in an EEA1-positive compartment in GCC88-depleted cells. HeLa A8 were treated with 10 ng/ml doxycycline for 72 h and then cotransfected with TGN38 alone (A and B) or with TGN38 and GFP-Rab7(Q67L) or GFP-Rab11wt (C), as indicated, 24 h before an internalization assay. Monolayers were incubated with monoclonal mouse anti-TGN38 antibodies for 30 min on ice, washed in PBS, and then incubated at 37°C in serum-free media for 120 min to internalize the antibody–TGN38 complex. Monolayers were fixed in 4% paraformaldehyde, permeabilized, and stained with Alexa568-conjugated anti-mouse IgG for 60 min. (A) Endogenous EEA1 was stained with human anti-EEA1 antibodies, followed by an FITC-conjugated anti-human IgG. (B) Magnification of the boxed image in A. The fluorescence intensity linescan profile was generated along the green line indicated in the merged panel, demonstrating the coincidence of the two fluorescent populations. Bars, 10 μm.

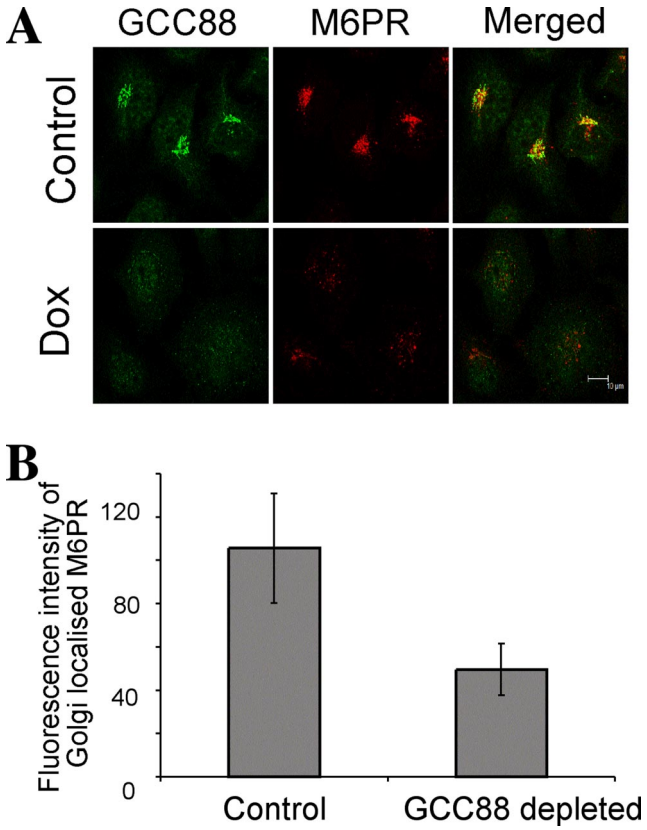

Figure 8. Intracellular distribution of endogenous CI-M6PR is disrupted in GCC88-depleted cells. (A) HeLa A8 were either untreated (control) or incubated in 10 ng/ml Dox for 96 h and then fixed in 4% paraformaldehyde and permeablized. Cell monolayers were stained with rabbit anti-GCC88 antibodies followed by Alexa488-conjugated anti-rabbit IgG, and monoclonal anti-M6PR followed by Alexa568-conjugated anti-mouse IgG. (B) For quantification of M6PR levels within the Golgi apparatus, fixed cell monolayers from A were stained with monoclonal anti-M6PR followed by Alexa568-conjugated anti-mouse IgG and rabbit anti-GMAP-210 followed by Alexa488-conjugated anti-rabbit IgG and analyzed for M6PR staining intensity within the Golgi, defined by the Golgi marker GMAP-210. Fluorescence intensity was quantified using Leica imaging software (n = 25). Results are means and error bars represent standard deviation ($P < 0.001$). Bars, 10 μm.

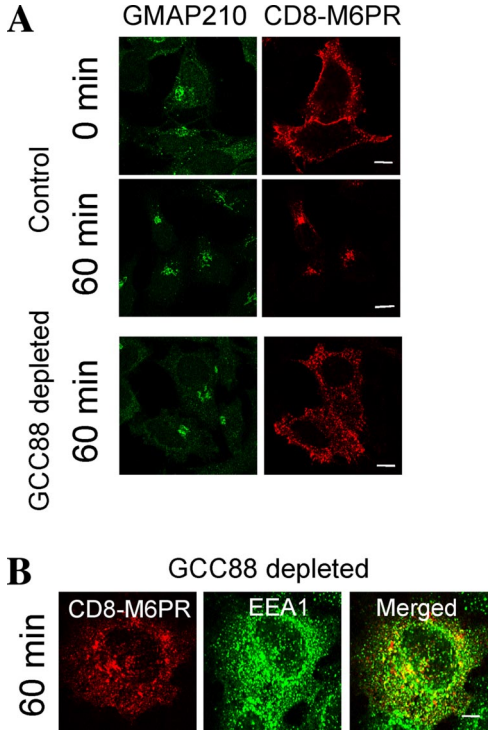

Figure 9. Trafficking of CD8-M6PR in GCC88 depleted cells. (A and B) HeLa A8 were either untreated (control) or incubated in 10 ng/ml doxycycline for 72 h (GCC88 depleted) and transfected with CD8-M6PR 24 h before an internalization assay. Transfected monolayers were incubated with monoclonal mouse anti-CD8α antibodies on ice for 30 min, washed in PBS, and then either fixed directly (0 min) or incubated in serum-free media for 60 min at 37°C. Monolayers were fixed in 4% paraformaldehyde, permeabilized, and stained with Alexa568-conjugated anti-mouse IgG for 60 min. Monolayers were stained with rabbit anti-GMAP-210 antibodies and Alexa488-conjugated anti-rabbit IgG. (B) Monolayers were also stained with human anti-EEA1 antibodies and Alexa647-conjugated antihuman IgG for 60 min. Bars, 10 μm.

CD8-M6PR from the plasma membrane, transfected HeLa A8 cells were labeled with anti-CD8 antibodies at 4°C and then incubated at various times at 37°C before fixation. In noninduced A8 cells, the CD8-M6PR chimera was first detected in the Golgi region by 30-min incubation at 37°C, and by 60 min the majority of the complex had been transported to the Golgi, consistent with the retrograde transport of the CI-M6PR (Figure 9A). In contrast, CD8-M6PR was not transported to the Golgi in GCC88-depleted cells over this period, but like TGN38 it remained in punctate endosomal structures, and the majority of these endosomal structures were EEA1 positive (Figure 9, A and B).

GCC88 Is Required for Syntaxin 6 Function

A possible explanation for the block in endosome to Golgi transport is GCC88 is required for the targeting and/or fusion of transport intermediates with the TGN. The molecular machinery involved in retrograde transport includes the t-SNAREs, syntaxin 6, syntaxin 16, and Vti1a that forms a functional complex with the endosomal v-SNARES, VAMP3, and VAMP4 (Mallard *et al.*, 2002); in particular, syntaxin 6 and VAMP4 have been implicated in recycling of TGN38 to the Golgi (Mallard *et al.*, 2002; Tran *et al.*, 2007). Therefore, we analyzed the localization of these SNAREs in GCC88-deficient cells to ascertain whether their steady-state intracellular distributions were affected by the absence of GCC88. Whereas VAMP3, VAMP4, syntaxin 16, and Vti1a showed similar intracellular distributions in control and GCC88-depleted cells, the distribution of syntaxin 6 was markedly perturbed in GCC88-depleted cells (Figure 10). In the majority (~75%) of GCC88-depleted cells syntaxin 6 showed a dispersed punctate cytoplasmic distribution and showed minimal localization to the Golgi region (Figure 10D). In contrast, a juxtanuclear Golgi localization of syntaxin 6 was detected in virtually all (97%) noninduced HeLa A8 cells; in these cells, syntaxin 6 showed extensive colocalization with p230/golgin-245, consistent with a TGN location of syntaxin 6 (Figure 10F). That not all GCC88-depleted cells show an altered syntaxin 6 localization could be due to residual low levels of GCC88-mediating syntaxin 6 localization. The Golgi localization of syntaxin 6 was not affected by depletion of p230/golgin-245 with siRNA (Figure 10F), demonstrating that the perturbation in syntaxin 6 localization was due to the specific absence of the golgin GCC88. The

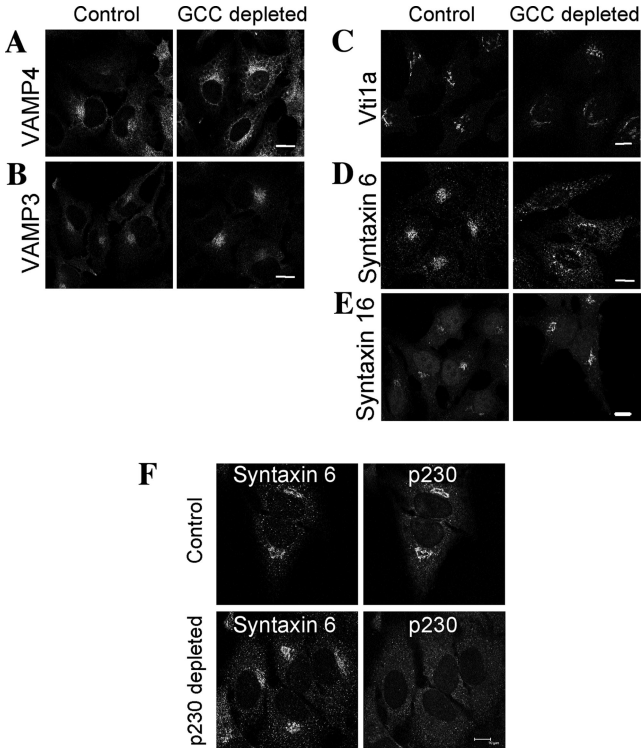

Figure 10. Depletion of GCC88 results in mislocalization of syntaxin 6. (A–E) HeLa A8 were either untreated (control) or incubated in 10 ng/ml doxycycline for 96 h (GCC88 depleted) and then fixed in 4% paraformaldehyde and permeablized. Fixed monolayers were stained for endogenous VAMP4 (A), VAMP3 (B), Vti1a (C), syntaxin 6 (D), and syntaxin 16 (E), with rabbit polyclonal antibodies to VAMP4, VAMP3, and syntaxin 16, respectively, followed by Alexa 568-conjugated rabbit IgG and mouse monoclonal antibodies to vti1a and syntaxin 6, respectively, followed by Alexa 568-conjugated anti-mouse IgG. (F) Untransfected HeLa cells (control) or HeLa cells transfected with p230 siRNA (p230 depleted) for 72 h were fixed in 4% paraformaldehyde and saponin permeabilized. Endogenous p230 was stained with human anti-p230 antibodies followed by FITC-conjugated anti-human IgG and syntaxin 6 stained with monoclonal mouse anti-syntaxin 6, followed by Alexa 568-conjugated anti-mouse IgG. Bars, 10 μm.

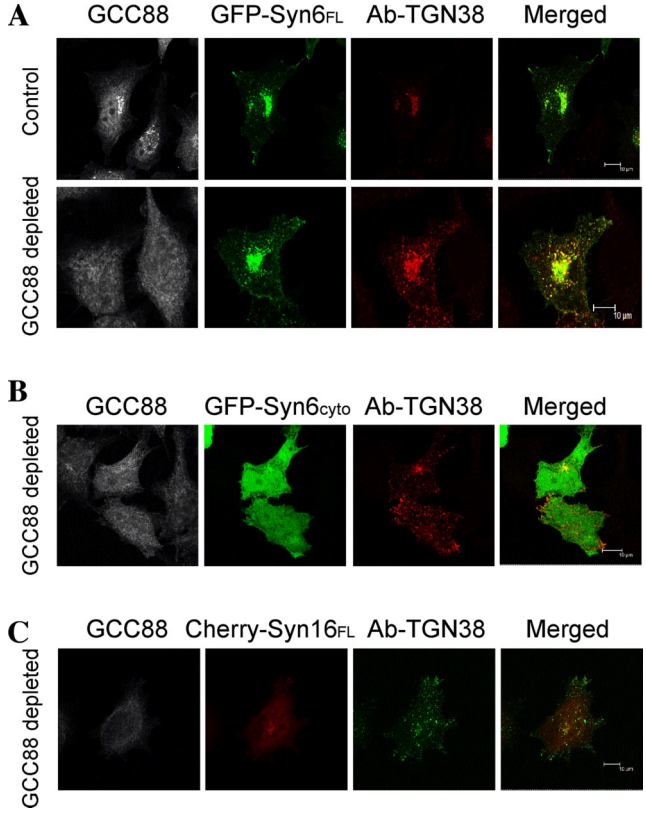

Figure 11. Defect in TGN38 recycling is rescued by expression of wild-type syntaxin 6. HeLa A8 were either untreated (control) or incubated in 10 ng/ml doxycycline for 96 h (GCC88 depleted) and cotransfected with TGN38 and either GFP-syntaxin6_{FL} (GFP-Syn6_{FL}) (A), GFP-syntaxin6_{cyto} (GFP-Syn6_{cyto}) (B), or cherry-syntaxin 16_{FL} (Cherry-Syn16_{FL}) (C) for 24 h before the internalization assay. Monolayers were incubated with monoclonal mouse anti-TGN38 antibodies for 30 min on ice, washed in PBS, and then incubated at 37°C in serum-free media 120 min to internalize the antibody–TGN38 complex. Monolayers were fixed in 4% paraformaldehyde, permeabilized, and stained with Alexa 568-conjugated anti-mouse IgG for 60 min. Endogenous GCC88 was stained with rabbit anti-GCC88 antibodies, followed by Alexa 647-conjugated anti-rabbit IgG. Cells with no GCC88 staining and perinuclear level of syntaxin 6 or syntaxin 16 expression were analyzed (n = 15, in duplicate). Bars, 10 μm.

precise location of syntaxin 6 in the GCC88-depleted cells was difficult to define as the syntaxin 6-positive cytoplasmic structures were negative for a variety of markers, including EEA1, rab11, and rab7 (data not shown). These results suggest that the TGN localization of syntaxin 6 is dependent on GCC88.

To investigate whether the redistribution of syntaxin 6 in GCC88-depleted cells is directly responsible for a block in retrograde transport, we then attempted to rescue the TGN38 trafficking defect in GCC88-depleted cells by the overexpression of syntaxin 6. HeLa A8 cells were treated with doxycycline for 96 h and then transfected with TGN38 together with either full-length syntaxin 6 (GFP-syntaxin 6_{FL}) or a truncated cytosolic form of syntaxin 6 (GFP-syntaxin 6_{cyto}), which is unable to participate in functional SNARE complexes (Mallard *et al.*, 2002). When expressed in HeLa cells, GFP-syntaxin 6_{FL} were targeted to the Golgi, as expected, whereas GFP-syntaxin 6_{cyto} was found predominantly in the cytosol (Figure 11, A and B). When expressed in GCC88-depleted cells GFP-syntaxin6_{FL} rescued the block in TGN38 trafficking in all cells analyzed (30/30), showing efficient trafficking of internalized TGN38–antibody complexes to the Golgi region (Figure 11A). In contrast, in HeLa A8 cells expressing GFP-syntaxin 6_{cyto} TGN38 remained accumulated in endosomal structures (Figure 11B). Therefore, expression of the full-length syntaxin 6, but not the truncated form of syntaxin 6 rescued the block in TGN38 trafficking, demonstrating that membrane bound syntaxin 6 is required to rescue the defect resulting from the absence of GCC88. The overexpression of a full-length unrelated Golgi syntaxin syntaxin 16 (cherry-Syn16_{FL}) also did not rescue the block in TGN38 trafficking (Figure 11C). These results demonstrate that GCC88 is required for the localization of endogenous syntaxin 6 within the Golgi to mediate efficient retrograde trafficking of cargo from the early endosomes.

Syntaxin 6 Is Required for Retrograde Transport of TGN38 but Not Shiga Toxin

In view of the relationship between GCC88 and syntaxin 6, we then directly analyzed the affect of syntaxin 6 depletion on retrograde transport. A dominant-negative mutant of

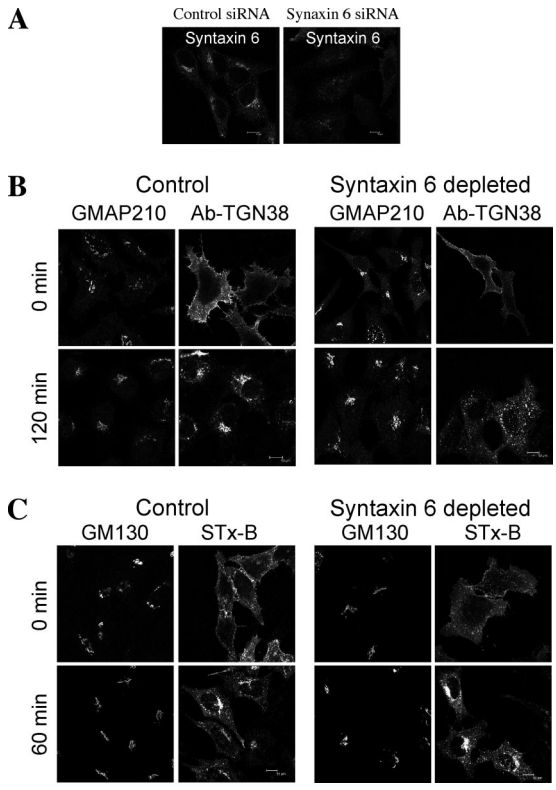

Figure 12. Syntaxin 6 depletion impairs TGN38, but not Shiga toxin, trafficking to the Golgi apparatus. (A) HeLa cells were transfected with syntaxin 6 siRNA for 72 h, fixed in 4% paraformaldehyde, saponin permeablized, and stained with monoclonal anti-syntaxin 6 antibodies followed by Alexa-conjugated mouse IgG. (B) HeLa cells transfected with siRNA as described above for 48 h, and then they were transfected a second time with CFP-TGN38 for a further 24 h. Monolayers were then incubated with monoclonal mouse anti-TGN38 antibodies on ice for 30 min, washed in PBS, and incubated in serum-free media at 37°C for 120 min. Monolayers were fixed in 4% paraformaldehyde, permeabilized, and stained with Alexa-conjugated anti-mouse IgG. Endogenous GMAP-210 was stained with rabbit anti-GMAP-210, followed by Alexa-conjugated anti-rabbit IgG. C) HeLa cells were transfected with syntaxin 6 siRNA for 72 h and incubated with Cy3-conjugated STx-B for 45 min on ice and then either fixed immediately (0 min) or incubated at 37°C for 60 min followed by fixation. Cells were stained with monoclonal antibodies to GM130 followed by Alexa 647-conjugated mouse IgG. Bars, 10 μm.

syntaxin 6 has previously been shown to partially perturb retrograde transport; however, the effect of silencing syntaxin 6 has not been examined. We identified a siRNA target for syntaxin 6, which was effective in reducing levels of syntaxin 6 in HeLa by >90% (Figure 12A; data not shown). In syntaxin 6 siRNA-transfected cells, internalized TGN38–antibody complexes were found predominantly in endosomal structures after 120 min at 37°C (Figure 12B), a result similar to that of GCC88 depletion. However, depletion of syntaxin 6 did not affect the retrograde transport of STx-B (Figure 12C). Using GMAP-210 staining to mark the Golgi region, we quantified the immunofluorescence intensity of the internalized STx-B that was located within the GM30-stained Golgi region (Supplemental Figure S4), and this analysis showed no difference in Golgi-localized STx-B between untreated and syntaxin 6–depleted cells. Therefore, silencing syntaxin 6 selectively impairs retrograde transport of TGN38, but not Shiga toxin, to the Golgi apparatus.

DISCUSSION

Analyzing the trafficking of cargo molecules such as TGN38 and Shiga toxin has identified retrograde transport pathways from endosomes to the TGN. The transport routes of these cargo to the TGN are considered to occur directly from the early endosome or via the recycling endosome; furthermore, it has been generally assumed that Shiga toxin and TGN38 share the same transport pathway and machinery (Sannerud *et al*., 2003). By combining internalization assays and single cell fluorescent analyses with RNAi-mediated silencing of TGN golgins, we have identified Golgi tethering molecules that independently regulate endosomal to TGN trafficking of these two cargoes.

TGN golgins, a group of peripheral coiled-coil membrane proteins with a GRIP targeting sequence, have previously been shown to play a role in defining the characteristics of TGN membranes (Gleeson *et al*., 2004). Two of the four TGN golgins, namely, p230/golgin-245 and golgin-97, are dependent on Arl1 for membrane recruitment (Gangi Setty *et al*., 2003; Lu and Hong, 2003; Panic *et al*., 2003a,b), whereas the other two TGN golgins, GCC88 and GCC185, do not bind to Arl1 in vivo, indicating differences in the membrane binding of the mammalian GRIP domain proteins, which likely reflects differences in function (Derby *et al*., 2007). Here, we have identified GCC88 as a key regulator of TGN38 and M6PR trafficking. By silencing GCC88 we have demonstrated that the transport of TGN38 and a CD8-M6PR chimera was blocked in the early endosome, whereas there was no affect on transport of STx-B to the Golgi. Recently, we demonstrated that the other Arl1-independent golgin, GCC185, is required for intracellular transport of internalized STx-B to the Golgi but that it had no affect on the retrograde transport of TGN38 (Derby *et al*., 2007); GCC185 depletion resulted an accumulation of Shiga toxin in Rab11-positive recycling endosomes. Thus, a major finding from our studies is the dissection of two independent retrograde transport pathways and the identification of Arl1-independent TGN golgins as key regulators of these retrograde transport pathways.

Silencing of GCC88 expression resulted in a block in retrograde transport. This phenotype was a specific consequence of the absence of GCC88 because 1) the silencing of GCC88 had no affect on the levels of the other TGN golgins; 2) staining for *cis*- and *trans*-Golgi markers showed no obvious perturbation in Golgi organization; 3) anterograde transport in GCC88-depleted cells was normal, indicating a functional Golgi apparatus; 4) independent shRNA and siRNA targets produced the same retrograde transport defect; 5) siRNA silencing of p230/golgin-245, golgin-97, or GCC185 did not result in a block in retrograde transport of TGN38; and 6) overexpression of exogenous full-length GCC88 rescued the transport defect in the RNAi-expressing cells. These results strongly argue that GCC88 is directly involved in retrograde transport.

In addition to a block in TGN38 recycling, we also showed that GCC88 depletion resulted in dispersal of endogenous M6PR throughout the cytoplasm and reduced levels within the Golgi region. Furthermore, by tracking the recycling of a CD8-M6PR chimera from the plasma membrane to the Golgi in GCC88-depleted cells, we demonstrated that the fusion protein was internalized, but it was blocked in retrograde transport, and, like TGN38, accumulated in early endosomes. Because both internalized TGN38 and the CD8-M6PR chimera, and also endogenous CI-M6PR, accumulated in an EEA1-positive compartment in GCC88-depleted cells, and because endogenous GCC88 is localized specifi-

cally to TGN membranes, these cargoes are likely to be transported directly from early endosomes to the TGN. In particular, a block in the docking of transport intermediates with the TGN would be expected to result in accumulation of the cargo in the penultimate compartment of the pathway, in this case the early endosome.

This study highlights the previously unappreciated complexity of the trafficking pathways used by the cargoes we have investigated. M6PR trafficking is complex and probably involves recycling to the TGN via a number of endosomal compartments, including early, recycling, and late endosomes (Ghosh *et al*., 2003; Bonifacino and Rojas, 2006). There is evidence that PACS-1/AP1 (Wan *et al*., 1998; Meyer *et al*., 2000; Scott *et al*., 2006) and retromer (Arighi *et al*., 2004; Carlton *et al*., 2004; Seaman, 2004; Rojas *et al*., 2007) mediate M6PR recycling from the early endosomes, whereas TIP47/Rab9 is involved in trafficking M6PR from the late endosomes (Diaz *et al*., 1997; Diaz and Pfeffer, 1998; Carroll *et al*., 2001; Reddy *et al*., 2006). The relative contribution of each pathway to the total M6P-R trafficking is yet to be determined. Our findings here suggest that the trafficking of the M6PR directly from the early endosome to the TGN in HeLa cells is likely to contribute significantly to the recycling of this receptor.

Recent studies have demonstrated that retromer and clathrin are also important in the transport of Shiga toxin (Saint-Pol *et al*., 2004; Bujny *et al*., 2007; Popoff *et al*., 2007; Utskarpen *et al*., 2007), and clathrin adaptors for the transport of TGN38 (Mallard *et al*., 1998; Saint-Pol *et al*., 2004), from early endosomes. For example, silencing components of the retromer complex, such as SNX1 and Vps26, resulted in the accumulation of Shiga toxin within the early endosome (Popoff *et al*., 2007). This approach elegantly defines the machinery required for exit from the early endosome but it does not delineate the precise pathway(s) used by these cargoes from the early endosome to the TGN. Alternatively, silencing components of the fusion machinery at the TGN provides a strategy to identify the final stages of retrograde transport and has potential to discriminate individual pathways. There is evidence for a role in various components of the fusion machinery for TGN38 and Shiga toxin transport to the Golgi, including Rab6A′, syntaxin 5, and syntaxin 16 (Mallard *et al*., 2002; Tai *et al*., 2004; Del Nery *et al*., 2006; Amessou *et al*., 2007), although the link between these components and the identity of the transport pathway(s) is not yet clear.

How does the TGN golgin GCC88 regulate endosome to TGN transport? GCC88 is a peripheral membrane protein localized specifically to TGN membranes, and the absence of this golgin could in theory inhibit either the generation of transport vesicles emerging from the TGN or the docking of transport carriers from the early endosome to the TGN. The outcome of either would be a block in transport between these two compartments due to the inability to recycle trafficking machinery. Our finding that GCC88 is required for Golgi retention of the t-SNARE syntaxin 6 suggests GCC88 has a role in regulating the fusion of transport intermediates delivered to the TGN.

The lack of GCC88 did not result in a complete block in TGN38 recycling. By 4-h internalization, the majority of TGN38 had been transported to the Golgi in GCC88 depleted cells, compared with 30 min in wild-type cells. The finding that the block in retrograde transport was only partial is consistent with the ability of HeLa A8 cells to grow for extended periods in the absence of this golgin. The TGN38 recycling that occurs in the absence of GCC88 could be due to the presence of low levels of syntaxin 6 in the TGN to allow transport, albeit at reduced rate, or by the use of an alternative transport pathway, such as via the recycling endosome or the late endosome.

There are at least two SNARE complexes involved in retrograde transport from the early/recycling endosomes to the TGN, a syntaxin 6 complex (Mallard *et al*., 2002) and a syntaxin 5 complex (Xu *et al*., 2002; Tai *et al*., 2004; Amessou *et al*., 2007). The retrograde transport pathways for these two SNARE complexes have yet to be defined. Previous work has indicated the importance of syntaxin 6 in TGN38 trafficking, because a dominant-negative cytosolic from of syntaxin 6 was shown to block the TGN transport of TGN38 (Mallard *et al*., 2002; Nakamura *et al*., 2005). Here, we found that GCC88 silencing resulted in the redistribution of syntaxin 6 from the Golgi to structures dispersed throughout the cytoplasm. The ability to rescue the trafficking defect in GCC88-depleted cells by the overexpression of exogenous syntaxin 6 shows a direct link between the mislocalization of this t-SNARE and the block in retrograde transport. Furthermore, using RNAi we have directly demonstrated that syntaxin 6 is required for the retrograde transport of TGN38, but not Shiga toxin, to the Golgi apparatus. Although syntaxin 6 has been previously linked to the trafficking of Shiga toxin, the study involved a reconstituted transport assay using permeabilized cells (Mallard *et al*., 2002). Our finding that depletion of syntaxin 6 has no apparent affect on retrograde transport in vivo raises the possibility that other SNARE complexes are involved. Indeed, the recent finding that silencing syntaxin 5 resulted in a block in Shiga toxin trafficking, and protection against intoxication by this toxin, (Amessou *et al*., 2007) highlights the possibility of multiple retrograde transport pathway by using different Golgi–SNARE complexes.

Ultrastructural studies have shown previously that syntaxin 6 is concentrated predominantly in the TGN in cell lines (Bock *et al*., 1997; Klumperman *et al*., 1998). There is evidence that syntaxin 6 recycles between the TGN and endosomes (Klumperman *et al*., 1998; Wendler and Tooze, 2001), in which case mechanisms must operate to retain syntaxin 6 in the TGN for a sufficient period to give a predominantly Golgi location under steady-state conditions. Our data suggest that GCC88 influences the retention of this t-SNARE in the TGN. We propose that an absence of GCC88 would result in poor retention of syntaxin 6 in the TGN, and a deficiency in this t-SNARE for the docking and fusion of transport intermediates. The ability of exogenous syntaxin 6 to rescue the transport defect in GCC88-depleted cells is consistent with this proposal, because overexpression of syntaxin 6 will increase the level of this t-SNARE in all compartments associated with the itinerary of syntaxin 6, including the TGN. Interestingly, another regulator of syntaxin 6 trafficking has been identified, namely, MARCH-II, which is considered to be an endosomal retention receptor (Nakamura *et al*., 2005), possibly reflecting the role of syntaxin 6 in a number of different transport pathways (Wendler and Tooze, 2001). In GCC88-depleted cells, syntaxin 6 was detected in cytoplasmic structures throughout the cytoplasm. The identity of these structures remains unclear, as these syntaxin 6-positive structures did not costain with a number of endosomal markers; however, further analyses of these structures may be useful in defining populations of transport intermediates.

There is a precedent for tethering molecules to influence the localization of SNAREs. p115 has been shown to interact with set of COPII vesicle-associated SNAREs (Allan *et al*., 2000) and the endosomal tethering molecule EEA1 interacts with t-SNARE syntaxin 13, the latter of which is required for

early endosomal fusion (McBride *et al*., 1999). Our study is the first example of a TGN tethering protein to influence the localization of a SNARE at the TGN. We have not been able to demonstrate a direct interaction between GCC88 and syntaxin 6, or another SNARE of the complex, namely, Vti1a, by immunoprecipitation (Lieu and Gleeson, unpublished data); however, this could be due to a transient interaction between the two molecules, as is the case for EEA1 and syntaxin 13 (McBride *et al*., 1999). Our earlier observation that overexpression of full-length GCC88 resulted in the generation of aberrant membrane structures, which excluded a number of TGN markers but included syntaxin 6 (Luke *et al*., 2003), again suggests a close relationship between these two membrane proteins.

In conclusion we have shown that the TGN golgin GCC88 is essential for efficient retrograde transport of a number of cargo proteins from the early endosome. The identity of a component involved in the fusion machinery at the TGN allows individual pathways to be blocked at the penultimate site of destination. Given that TGN38 accumulates in early endosomes, and there is a redistribution of syntaxin 6 as a consequence of GCC88 depletion, we propose that GCC88 is an effector molecular to mediate the recruitment of SNARE molecules required for the docking and fusion of transport intermediates derived from the early endosomes. The silencing of TGN golgins has the potential to provide a more sensitive discrimination of the retrograde transport pathways than the silencing of promiscuous SNAREs such as syntaxin 5 and syntaxin 6, which may perturb multiple pathways (Hay *et al*., 1998; Wendler and Tooze, 2001; Xu *et al*., 2002; Tai *et al*., 2004). The identification of the two TGN golgins GCC88 and GCC185 that independently regulate the trafficking of TGN38 and Shiga toxin, respectively, highlights the complexity of the retrograde transport pathways and provides the ability to define these pathways in more detail.

ACKNOWLEDGMENTS

We thank Michelle Bornens, Bruno Goud, Wanjin Hong, and Derek Toomre (Yale University) for reagents, and Fiona Houghton for expert technical advice and assistance. Z.Z.L. is supported by an Australian Postgraduate Award. R.D.T. is supported by a National Health and Medical Research Council R. Douglas Wright Career Development Award. This work was supported by funding from the Australian Research Council.

REFERENCES

Allan, B. B., Moyer, B. D., and Balch, W. E. (2000). Rab1 recruitment of p115 into a cis-SNARE complex: Programming budding COPII vesicles for fusion. Science *289*, 444–448.

Amessou, M., Fradagrada, A., Falguieres, T., Lord, J. M., Smith, D. C., Roberts, L. M., Lamaze, C., and Johannes, L. (2007). Syntaxin 16 and syntaxin 5 are required for efficient retrograde transport of several exogenous and endogenous cargo proteins. J. Cell Sci. *120*, 1457–1468.

Arighi, C. N., Hartnell, L. M., Aguilar, R. C., Haft, C. R., and Bonifacino, J. S. (2004). Role of the mammalian retromer in sorting of the cation-independent mannose 6-phosphate receptor. J. Cell Biol. *165*, 123–133.

Barr, F. A. (1999). A novel Rab6-interacting domain defines a family of Golgi-targeted coiled-coil proteins. Curr. Biol. *9*, 381–384.

Bock, J. B., Klumperman, J., Davanger, S., and Scheller, R. H. (1997). Syntaxin 6 functions in trans-Golgi network vesicle trafficking. Mol. Biol. Cell *8*, 1261–1271.

Bonifacino, J. S., and Rojas, R. (2006). Retorgrade transport from endosomes to the trans-Golgi network. Nat. Rev. Mol. Cell Biol. *7*, 568–579.

Bujny, M. V., Popoff, V., Johannes, L., and Cullen, P. J. (2007). The retromer component sorting nexin-1 is required for efficient retrograde transport of Shiga toxin from early endosome to the trans Golgi network. J. Cell Sci. *120*, 2010–2021.

Cai, H., Zhang, Y., Pypaert, M., Walker, L., and Ferro-Novick, S. (2005). Mutants in trs120 disrupt traffic from the early endosome to the late Golgi. J. Cell Biol. *171*, 823–833.

Carlton, J., Bujny, M., Peter, B. J., Oorschot, V. M., Rutherford, A., Mellor, H., Klumperman, J., McMahon, H. T., and Cullen, P. J. (2004). Sorting nexin-1 mediates tubular endosome-to-TGN transport through coincidence sensing of high-curvature membranes and 3-phosphoinositides. Curr. Biol. *14*, 1791–1800.

Carroll, K. S., Hanna, J., Simon, I., Krise, J., Barbero, P., and Pfeffer, S. R. (2001). Role of Rab9 GTPase in facilitating receptor recruitment by TIP47. Science *292*, 1373–1376.

Del Nery, E., Miserey-Lenkei, S., Falguieres, T., Nizak, C., Johannes, L., Perez, F., and Goud, B. (2006). Rab6A and Rab6A′ GTPases play non-overlapping roles in membrane trafficking. Traffic *7*, 394–407.

Derby, M. C., Lieu, Z. Z., Brown, D., Stow, J. L., Goud, B., and Gleeson, P. A. (2007). The trans-Golgi network golgin, GCC185, is required for endosome-to-Golgi transport and maintenance of Golgi structure. Traffic *8*, 758–773.

Derby, M. C., van Vliet, C., Brown, D., Luke, M. R., Lu, L., Hong, W., Stow, J. L., and Gleeson, P. A. (2004). Mammalian GRIP domain proteins differ in their membrane binding properties and are recruited to distinct domains of the TGN. J. Cell Sci. *117*, 5865–5874.

Diaz, E., and Pfeffer, S. R. (1998). TIP *47*, a cargo selection device for mannose 6-phosphate receptor trafficking. Cell *93*, 433–443.

Diaz, E., Schimmoller, F., and Pfeffer, S. R. (1997). A novel Rab9 effector required for endosome-to-TGN transport. J. Cell Biol. *138*, 283–290.

Erlich, R., Gleeson, P. A., Campbell, P., Dietzsch, E., and Toh, B. H. (1996). Molecular characterization of trans-Golgi p230: a human peripheral membrane protein encoded by a gene on chromosome 6p12–22 contains extensive coiled-coil alpha-helical domains and a granin motif. J. Biol. Chem. *271*, 8328–8337.

Fritzler, M. J., Lung, C. C., Hamel, J. C., Griffith, K. J., and Chan, E.K.L. (1995). Molecular characterization of golgin-245, a novel Golgi complex protein containing a granin signature. J. Biol. Chem. *270*, 31262–31268.

Gangi Setty, S. R., Shin, M. E., Yoshino, A., Marks, M. S., and Burd, C. G. (2003). Golgi recruitment of GRIP domain proteins by Arf-like GTPase 1 is regulated by Arf-like GTPase 3. Curr. Biol. *13*, 401–404.

Ghosh, P., Dahms, N. M., and Kornfeld, S. (2003). Mannose 6-phosphate receptors: new twists in the tale. Nat. Rev. Mol. Cell Biol. *4*, 202–212.

Ghosh, R. N., Mallet, W. G., Soe, T. T., McGraw, T. E., and Maxfield, F. R. (1998). An endocytosed TGN38 chimeric protein is delivered to the TGN after trafficking through the endocytic recycling compartment in CHO cells. J. Cell Biol. *142*, 923–936.

Gleeson, P. A., Anderson, T. J., Stow, J. L., Griffiths, G., Toh, B. H., and Matheson, F. (1996). p230 is associated with vesicles budding from the trans-Golgi network. J. Cell Sci. *109*, 2811–2821.

Gleeson, P. A., Lock, J. G., Luke, M. R., and Stow, J. L. (2004). Domains of the TGN: coats, tethers and G proteins. Traffic *5*, 315–326.

Gossen, M., and Bujard, H. (1992). Tight control of gene expression in mammalian cells by tetracycline-responsive promoters. Proc. Natl. Acad. Sci. USA *89*, 5547–5551.

Griffith, K. J., Chan, E.K.L., Lung, C. C., Hamel, J. C., Guo, X. Y., Miyachi, K., and Fritzler, M. J. (1997). Molecular cloning of a novel 97-Kd Golgi complex autoantigen associated with Sjogrens-syndrome. Arthritis Rheum. *40*, 1693–1702.

Hay, J. C., Klumperman, J., Oorschot, V., Steegmaier, M., Kuo, C. S., and Scheller, R. H. (1998). Localization, dynamics, and protein interactions reveal distinct roles for ER and Golgi SNAREs. J. Cell Biol. *141*, 1489–1502.

Infante, C., Ramos-Morales, F., Fedriani, C., Bornens, M., and Rios, R. M. (1999). GMAP-210, A cis-Golgi network-associated protein, is a minus end microtubule-binding protein. J. Cell Biol. *145*, 83–98.

Jackson, C. L. (2003). Membrane traffic: Arl GTPases get a GRIP on the Golgi. Curr. Biol. *13*, R174–R176.

Kakinuma, T., Ichikawa, H., Tsukada, Y., Nakamura, T., and Toh, B. H. (2004). Interaction between p230 and MACF1 is associated with transport of a glycosyl phosphatidyl inositol-anchored protein from the Golgi to the cell periphery. Exp. Cell Res. *298*, 388–398.

Keller, P., Toomre, D., Diaz, E., White, J., and Simons, K. (2001). Multicolour imaging of post-Golgi sorting and trafficking in live cells. Nat. Cell Biol. *3*, 140–149.

Kjer-Nielsen, L., Teasdale, R. D., van Vliet, C., and Gleeson, P. A. (1999a). A novel Golgi-localisation domain shared by a class of coiled-coil peripheral membrane proteins. Curr. Biol. *9*, 385–388.

Kjer-Nielsen, L., van Vliet, C., Erlich, R., Toh, B. H., and Gleeson, P. A. (1999b). The Golgi-targeting sequence of the peripheral membrane protein p230. J. Cell Sci. *112*, 1645–1654.

Klumperman, J., Kuliawat, R., Griffith, J. M., Geuze, H. J., and Arvan, P. (1998). Mannose 6-phosphate receptors are sorted from immature secretory granules via adaptor protein AP-1, clathrin, and syntaxin 6-positive vesicles. J. Cell Biol. *141*, 359–371.

Kooy, J., Toh, B. H., Pettitt, J. M., Erlich, R., and Gleeson, P. A. (1992). Human autoantibodies as reagents to conserved Golgi components: characterization of a peripheral, 230-kDa compartment-specific Golgi protein. J. Biol. Chem. *267*, 20255–20263.

Lewis, M. J., Nichols, B. J., Prescianotto-Baschong, C., Riezman, H., and Pelham, H. R. (2000). Specific retrieval of the exocytic SNARE Snc1p from early yeast endosomes. Mol. Biol. Cell *11*, 23–38.

Lock, J. G., Hammond, L. A., Houghton, F., Gleeson, P. A., and Stow, J. L. (2005). E-cadherin transport from the trans-Golgi network in tubulovesicular carriers is selectively regulated by golgin-97. Traffic *6*, 1142–1156.

Lock, J. G., and Stow, J. L. (2005). Rab11 in recycling endosomes regulates the sorting and basolateral transport of E-cadherin. Mol. Biol. Cell *16*, 1744–1755.

Lu, L., and Hong, W. (2003). Interaction of Arl1-GTP with GRIP domains recruits autoantigens Golgin-97 and Golgin-245/p230 onto the Golgi. Mol. Biol. Cell *14*, 3767–3781.

Lu, L., Tai, G., and Hong, W. (2004). Autoantigen Golgin-97, an effector of Arl1 GTPase, participates in traffic from the endosome to the TGN. Mol. Biol. Cell *15*, 4426–4443.

Luke, M. R., Houghton, F., Perugini, M. A., and Gleeson, P. A. (2005). The trans-Golgi network GRIP-domain proteins form alpha-helical homodimers. Biochem. J. *388*, 835–841.

Luke, M. R., Kjer-Nielsen, L., Brown, D. L., Stow, J. L., and Gleeson, P. A. (2003). GRIP domain-mediated targeting of two new coiled-coil proteins, GCC88 and GCC185, to subcompartments of the trans-Golgi network. J. Biol. Chem. *278*, 4216–4226.

Mallard, F., Antony, C., Tenza, D., Salamero, J., Goud, B., and Johannes, L. (1998). Direct pathway from early/recycling endosomes to the Golgi apparatus revealed through the study of shiga toxin B-fragment transport. J. Cell Biol. *143*, 973–990.

Mallard, F., Tang, B. L., Galli, T., Tenza, D., Saint-Pol, A., Yue, X., Antony, C., Hong, W., Goud, B., and Johannes, L. (2002). Early/recycling endosomes-to-TGN transport involves two SNARE complexes and a Rab6 isoform. J. Cell Biol. *156*, 653–664.

McBride, H. M., Rybin, V., Murphy, C., Giner, A., Teasdale, R., and Zerial, M. (1999). Oligomeric complexes link Rab5 effectors with NSF and drive membrane fusion via interactions between EEA1 and syntaxin 13. Cell *98*, 377–386.

Meyer, C., Zizioli, D., Lausmann, S., Eskelinen, E. L., Hamann, J., Saftig, P., von Figura, K., and Schu, P. (2000). mu 1A-adaptin-deficient mice: lethality, loss of AP-1 binding and rerouting of mannose 6-phosphate receptors. EMBO J. *19*, 2193–2203.

Mu, F. T., Callaghan, J. M., Steele-Mortimer, O., Stenmark, H., Parton, R. G., Campbell, P. L., McCluskey, J., Yeo, J. P., Tock, E. P., and Toh, B. H. (1995). EEA1, an early endosome-associated protein. EEA1 is a conserved alpha-helical peripheral membrane protein flanked by cysteine "fingers" and contains a calmodulin-binding IQ motif. J. Biol. Chem. *270*, 13503–13511.

Munro, S., and Nichols, B. J. (1999). The GRIP domain–a novel Golgi-targeting domain found in several coiled-coil proteins. Curr. Biol. *9*, 377–380.

Nakamura, N., Fukuda, H., Kato, A., and Hirose, S. (2005). MARCH-II is a syntaxin-6-binding protein involved in endosomal trafficking. Mol. Biol. Cell *16*, 1696–1710.

Panic, B., Perisic, O., Veprintsev, D. B., Williams, R. L., and Munro, S. (2003a). Structural basis for Arl1-dependent targeting of homodimeric GRIP domains to the Golgi apparatus. Mol. Cell *12*, 863–874.

Panic, B., Whyte, J. R., and Munro, S. (2003b). The ARF-like GTPases Arl1p and Arl3p act in a pathway that interacts with vesicle-tethering factors at the Golgi apparatus. Curr. Biol. *13*, 405–410.

Popoff, V., Mardones, G. A., Tenza, D., Rojas, R., Lamaze, C., Bonifacino, J. S., Raposo, G., and Johannes, L. (2007). The retromer complex and clathrin define an early endosomal retrograde exit site. J. Cell Sci. *120*, 2022–2031.

Reddy, J. V., Burguete, A. S., Sridevi, K., Ganley, I. G., Nottingham, R. M., and Pfeffer, S. R. (2006). A functional role for the GCC185 golgin in mannose 6-phosphate receptor recycling. Mol. Biol. Cell *17*, 4353–4363.

Rojas, R., Kametaka, S., Haft, C. R., and Bonifacino, J. S. (2007). Interchangeable but essential functions of SNX1 and SNX2 in the association of retromer with endosomes and the trafficking of mannose 6-phosphate receptors. Mol. Cell Biol. *27*, 1112–1124.

Saint-Pol, A. *et al*. (2004). Clathrin adaptor epsinR is required for retrograde sorting on early endosomal membranes. Dev. Cell *6*, 525–538.

Sandvig, K., and van Deurs, B. (2005). Delivery into cells: lessons learned from plant and bacterial toxins. Gene Ther. *12*, 865–872.

Sannerud, R., Saraste, J., and Goud, B. (2003). Retrograde traffic in the biosynthetic-secretory route: pathways and machinery. Curr. Opin. Cell Biol. *15*, 438–445.

Scott, G. K., Fei, H., Thomas, L., Medigeshi, G. R., and Thomas, G. (2006). A PACS-1, GGA3 and CK2 complex regulates CI-MPR trafficking. EMBO J. *25*, 4423–4435.

Seaman, M. N. (2004). Cargo-selective endosomal sorting for retrieval to the Golgi requires retromer. J. Cell Biol. *165*, 111–122.

Shewan, A. M., van Dam, E. M., Martin, S., Luen, T. B., Hong, W., Bryant, N. J., and James, D. E. (2003). GLUT4 recycles via a trans-Golgi network (TGN) subdomain enriched in Syntaxins 6 and 16 but not TGN *38*, involvement of an acidic targeting motif. Mol. Biol. Cell *14*, 973–986.

Stanley, K. K., and Howell, K. E. (1993). TGN38/ *41*, a molecule on the move. Trends Cell Biol. *3*, 252–255.

Tai, G., Lu, L., Wang, T. L., Tang, B. L., Goud, B., Johannes, L., and Hong, W. (2004). Participation of the syntaxin 5/Ykt6/GS28/GS15 SNARE complex in transport from the early/recycling endosome to the trans-Golgi network. Mol. Biol. Cell *15*, 4011–4022.

Tran, T. H., Zeng, Q., and Hong, W. (2007). VAMP4 cycles from the cell surface to the trans-Golgi network via sorting and recycling endosomes. J. Cell Sci. *120*, 1028–1041.

Tsukada, M., Will, E., and Gallwitz, D. (1999). Structural and functional analysis of a novel coiled coil protein involved in Ypt6 GTPase-regulated protein transport in yeast. Mol. Biol. Cell *10*, 63–75.

Ungar, D., Oka, T., Krieger, M., and Hughson, F. M. (2006). Retrograde transport on the COG railway. Trends Cell Biol. *16*, 113–120.

Utskarpen, A., Slagsvold, H. H., Dyve, A. B., Skanland, S. S., and Sandvig, K. (2007). SNX1 and SNX2 mediate retrograde transport of Shiga toxin. Biochem. Biophys. Res. Commun. *358*, 566–570.

Wan, L., Molloy, S. S., Thomas, L., Liu, G., Xiang, Y., Rybak, S. L., and Thomas, G. (1998). PACS-1 defines a novel gene family of cytosolic sorting proteins required for trans-Golgi network localization. Cell *94*, 205–216.

Watson, R. T., and Pessin, J. E. (2000). Functional cooperation of two independent targeting domains in syntaxin 6 is required for its efficient localization in the *trans*-Golgi network of 3T3L1 adipocytes. J. Biol. Chem. *275*, 1261–1268.

Wendler, F., and Tooze, S. (2001). Syntaxin *6*, the promiscuous behaviour of a SNARE protein. Traffic *2*, 606–611.

Wilcke, M., Johannes, L., Galli, T., Mayau, V., Goud, B., and Salamero, J. (2000). Rab11 regulates the compartmentalization of early endosomes required for efficient transport from early endosomes to the trans-Golgi network. J. Cell Biol. *151*, 1207–1220.

Xu, Y., Martin, S., James, D. E., and Hong, W. (2002). GS15 forms a SNARE complex with syntaxin 5, GS28, and Ykt6 and is implicated in traffic in the early cisternae of the Golgi apparatus. Mol. Biol. Cell *13*, 3493–3507.

Yoshino, A. *et al*. (2005). tGolgin-1 (p230, golgin-245) modulates Shiga-toxin transport to the Golgi and Golgi motility towards the microtubule-organizing centre. J. Cell Sci. *118*, 2279–2293.

Zhang, X. M., Ellis, S., Sriratana, A., Mitchell, C. A., and Rowe, T. (2004). Sec15 is an effector for the Rab11 GTPase in mammalian cells. J. Biol. Chem. *279*, 43027–43034.